Industrial crude bioethanol dehydration to ethylene: Doping ZSM-5 to enhance selectivity and stability

Eliana Quiroga, Nicolas García, Bernay Cifuentes, Ricardo Cogua, Jorge Becerra, Julia Moltó Berenguer, Martha Cobo

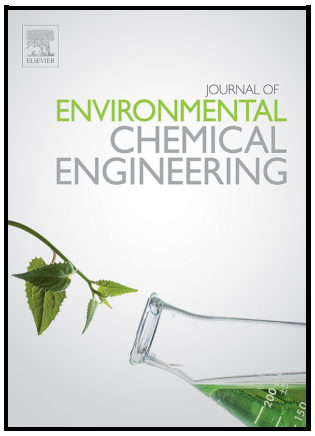

PII: S2213-3437(23)02542-3

DOI: https://doi.org/10.1016/j.jece.2023.111803

Reference: JECE111803

To appear in: *Journal of Environmental Chemical Engineering*

Received date: 17 May 2023
Revised date: 1 December 2023
Accepted date: 22 December 2023

Please cite this article as: Eliana Quiroga, Nicolas García, Bernay Cifuentes, Ricardo Cogua, Jorge Becerra, Julia Moltó Berenguer and Martha Cobo, Industrial crude bioethanol dehydration to ethylene: Doping ZSM-5 to enhance selectivity and stability, *Journal of Environmental Chemical Engineering,* (2023) doi:https://doi.org/10.1016/j.jece.2023.111803

Industrial crude bioethanol dehydration to ethylene: Doping ZSM-5 to enhance selectivity and stability

Eliana Quiroga[1,5], Nicolas García[1], Bernay Cifuentes[2], Ricardo Cogua[1], Jorge Becerra[3], Julia Moltó Berenguer[4,5], and Martha Cobo[1]*

[1]Energy, Materials and Environment Laboratory, Universidad de La Sabana, Campus Universitario Puente del Común, km. 7 Autopista Norte, Bogotá, Colombia

[2]Faculty of Engineering, Chemical Engineering, Universidad de La Salle, Bogotá, Carrera 2 # 10-70, Bogotá, Colombia.

[3]SNC-Lavalin, 5500 boul. des Galeries, Québec (QC), Canada, G2K 2E2.

[4]Department of Chemical Engineering, University of Alicante, P.O. Box 99, E-03080, Alicante, Spain

[5]Institute of Chemical Process Engineering, University of Alicante, P.O. Box 99, E-03080, Alicante, Spain

*Corresponding author: Email: martha.cobo@unisabana.edu.co, Tel: +571 8615555 Ext. 25211, Fax: +571 8615555

Declarations of interest:
none

Abstract

Although the conversion of bioethanol into light olefins is one of the most studied processes in biorefinery schemes, there is a need to develop materials more capable of operating at industrial conditions (WHSV > 20 h^{-1} crude bioethanol feed). Hence, in this

study, we dehydrated crude bioethanol samples derived from sugarcane fermentation to produce ethylene over a series of H-ZSM-5 zeolites. Among them, H-ZSM-5 with different Si/Al ratios (26, 280, and 371) and doped with Ce and Cu were tested on the catalytic activity and stability. Accordingly, a 26 Si/Al ratio showed full conversion and ethylene selectivity at 300 °C with a WHSV of 30.2 h^{-1}. When doping the zeolites, a decrease in relative crystallinity and a higher amount of acid sites were observed, which affected the interaction with reactants. This interaction was deeply analyzed by the *in-situ* DRIFTS, which showed that ethanol adsorption is lower for doped zeolites, but the desorption rate is higher, showing higher stability over longer reaction times. Therefore, the H-ZSM-5 with a Si/Al ratio of 26 and doped with Ce maintained its activity and improved its selectivity over 140 h under more drastic conditions of WHSV (42.3 h^{-1}). These results elucidate that Ce-doped H-ZSM-5 zeolites can improve stability and represent a starting point for large-scale crude bioethanol conversion.

Keywords:

Bioethylene production; Biorefinery; Dopants; *in-situ* DRIFTS; Light olefins.

1. Introduction

The transition from traditional fossil-based to clean and innovative production is necessary to address climate change and ensure a sustainable future [1]. In this way, one of the alternatives are biorefineries, which can produce biofuels (e.g., hydrogen, bioethanol, and biodiesel), bioproducts (e.g., detergents, additives, fibers, and adhesives), and chemicals (e.g., acids, alcohols, and olefins) from renewable sources such as biomass [2]. Most of the commercial biorefineries have focused on the production of biofuels [3], leaving behind the

production of bioproducts and chemicals from biomass, which is also necessary to ensure a low-carbon development.

One of the most widely used chemicals in the world is ethylene (C_2H_4), it is used in the production of polymers, refrigerants, medicines, fibers, and fertilizers as well as in the thermal cutting and pulverization of metals [4]. C_2H_4 is the most commercialized organic compound in the world, reaching an annual demand of 168 Mt in 2020 with a projected growth of 3% per year [5] and a selling price of USD 1,235 t^{-1} in the next decade [6]. However, C_2H_4 is conventionally produced through the catalytic cracking of naphtha with steam at temperatures above 700 °C [4]. Thus, the conventional process to produce C_2H_4 consumes a great amount of energy (94.95 GJ t $C_2H_4^{-1}$), emits CO_2 (1.47 t CO_2 t $C_2H_4^{-1}$) [7], and uses fossil resources (i.e., naphtha) [8]. Therefore, it is urgent to implement sustainable alternatives for its production.

A sustainable route to obtain olefins such as C_2H_4 is the catalytic dehydration of bioethanol [9]. Thus, the implementation of this process makes it possible to take advantage of the existing infrastructure for the production of biofuels [4]. Bioethanol is one of the main biofuels produced; around 25 billion gallons per year are produced worldwide [10]. For instance, in Colombia around 346 thousand tons of bioethanol are produced per year with a sale price of USD 760 t^{-1} [11]. Likewise, a growth of up to 23% in the production of bioethanol is expected [11], driven by the energy transition [12]. Currently, bioethanol is blended with other fuels, thus a high purity is required. For this reason, bioethanol production plants have dehydration processes to increase the purity of the desired product coming from the top of the distillation column. These processes generate greater energy consumption, and involve additional infrastructure costs [13–15]. However, it is expected that after 2030, gasoline-powered vehicles will start to be replaced by electric and

hydrogen-powered ones [16], gradually releasing bioethanol for used in other applications including the manufacture of industrial chemicals. We recently evaluated [17] the technical-economic feasibility of implementing olefin production plants from ethanol in Colombia, with capacities of up to 13.9 Mt year^{-1} of C_2H_4. It was found that the required investments are similar to those of the conventional petrochemical industry (i.e., Capex of 1 million USD and Opex of 4.7 million USD per year [17]), while producing a lower environmental impact. Thus, the production of C_2H_4 from bioethanol could be a promising step in the Colombian strategy which aims at the development of sustainable chemical production models.

Obtaining C_2H_4 from ethanol is a well-known process, where the type of bioethanol, space velocity, temperature, and catalyst are the most important variables to industrially scale up the process. Research on ethanol dehydration for olefins production has been carried out using mainly synthetic bioethanol (i.e., a mixture of anhydrous ethanol and distilled water) [18–20]. However, bioethanol from biomass fermentation contains several impurities, including alcohols (i.e., propanol, butanol, pentanol), aldehydes, amines, acids, and esters [21]. Removing these impurities (i.e., produce anhydrous ethanol) requires a simple distillation followed by rigorous purification processes, such as vacuum distillation or the use of molecular sieves, which considerably increase the cost of bioethanol (up to 5 times more expensive) [17]. Therefore, the industrial implementation of C_2H_4 production is expected to be achieved using crude bioethanol (i.e., without rigorous purifications). However, it has been reported that the presence of impurities in crude bioethanol affects the catalytic performance during ethanol chemical conversion processes [21]. Sanchez et al. [22] studied ethanol reforming over Rh-Pt/CeO_2-SiO_2 catalysts with bioethanol obtained from non-centrifugal sugarcane agroindustry, reporting that the presence of impurities such

as 3-methyl-1-butanol favored the formation of long-chain carbonaceous compounds, leading to early catalyst deactivation. Shetsiri et al. studied the production of C_2H_4 on hierarchical ZSM-5 nanosheets, finding that the catalyst is rapidly deactivated when using crude bioethanol (from sugar cane and cassava chips) compared to synthetic bioethanol [23]. In addition, studies conducted with crude bioethanol samples have been carried out with low weight hourly space velocity (WHSV) values of 2 h^{-1} [18] or 0.81 h^{-1} [19], which implies a higher amount of catalyst to achieve higher yields at C_2H_4 [18,19]. Although the authors do not elaborate on this result because the objective of their paper was to evaluate the effect of catalyst doping, these results highlight the need to address the effect of using crude bioethanol samples on the catalytic performance during ethanol dehydration to produce C_2H_4.

Zeolites of type H-ZSM-5 are the most studied materials for this reaction, as they can achieve ethanol conversion and selectivity to C_2H_4 > 95% [24]. This is due to its thermal stability, microcrystalline structure, and superior cation exchange capacity, which favor the dehydration of alcohols [25]. In a previous report, our research group obtained ethanol conversion and selectivity to C_2H_4 of 99% in the dehydration of synthetic ethanol samples using H-ZSM-5 zeolites with different Si/Al ratios (Si/Al = 23, 30, and 280) in a fixed-bed reactor at 300 °C [17]. Moreover, Chae et al. [18] evaluated the dehydration of ethanol over Lanthanum (La)-doped H-ZSM-5 (Si/Al = 23) zeolites, obtaining that doping with La maintained the conversion > 90% and increased the selectivity to C_2H_4 by 10%, improving the stability of the zeolite [18]. In fact, it is accepted that doping H-ZSM-5 zeolites with Fe [19,26], Ni, P [26], Cu [27], and Ce [28] for the production of olefins from alcohols could improve selectivity because it decreases the formation of Brønsted acids, which lead to the

formation of coke [26,27]. Thus, H-ZSM-5 zeolites, with or without doping, stand out as promising catalysts for obtaining C_2H_4 from ethanol.

Therefore, the purpose of this contribution was to study the catalytic performance of H-ZSM-5 zeolites in the dehydration of crude bioethanol containing impurities and coming from industrial sugarcane processing plants in Colombia. For this purpose, catalytic activity studies were carried out on H-ZSM-5 zeolites with a Si/Al ratio =26, 280, and 371, some doped with Ce and Cu, at different temperatures. Several characterization techniques were used to evaluate the effect of the dopants on acidity and crystallinity of the zeolites; as well as the type and stability of the adsorbed species. In addition, the stability of the most active catalysts was evaluated through 140 h time on stream (TOS) at two different operating temperatures.

2. Materials and methods

2.1. Characterization of bioethanol samples

Bioethanol samples were obtained from the production plant of a sugar mill (Palmira, Colombia). Figure 1 shows the bioethanol production process, which begins with the reception of residual juice from sugar production. This juice is fed to a fermenter (E-1) to obtain a must containing water, ethanol, other alcohols, and yeast. After recovering the yeast by decantation (E-2), the resulting wine is taken to a distillation column (E-5) to purify the bioethanol. Four raw bioethanol streams of different purities were obtained in this tower. The fraction obtained from the "medium" was separated by decantation (E-7) to obtain two samples: Light Medium and Heavy Medium. The concentration of the compounds present (i.e., ethanol, propanol, butanol, pentanol, and water) in each bioethanol sample was analyzed by gas chromatography (GC) on a Clarus 580 unit (Perkin Elmer,

USA), equipped with an HP-PLOT column (Agilent, USA) connected to a flame ionization detector (FID).

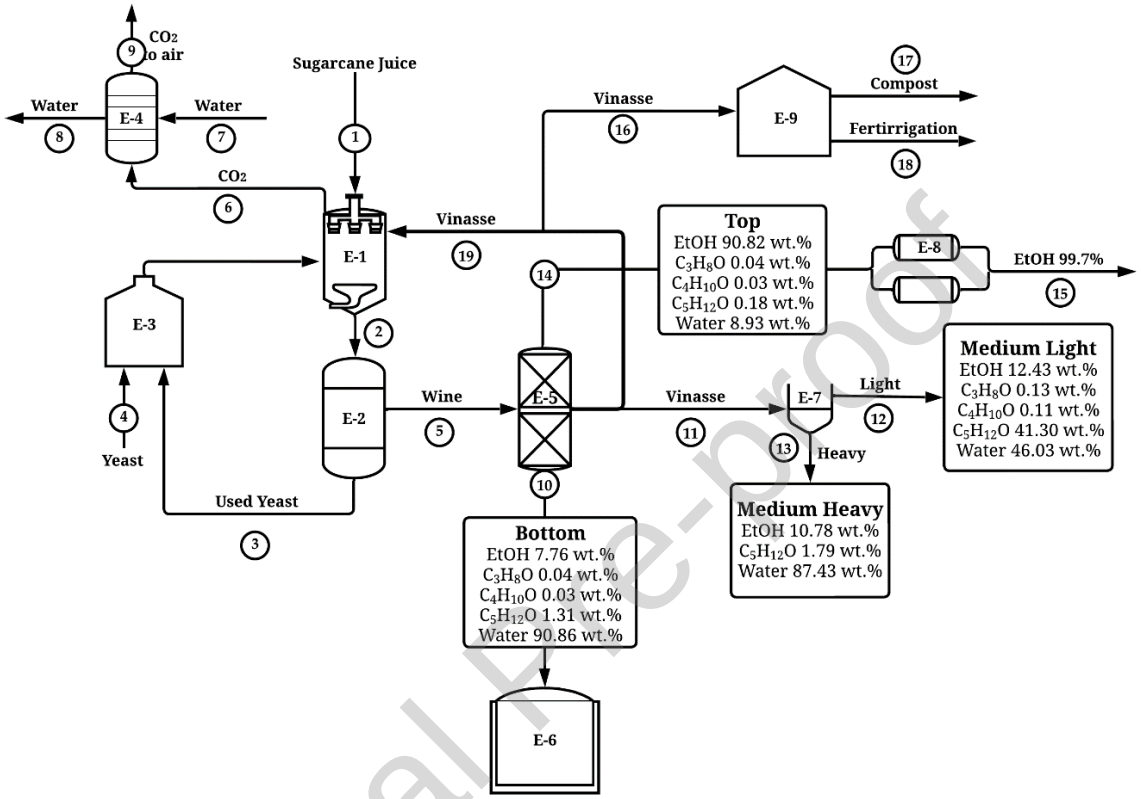

Figure 1. Bioethanol production process at the sugar mill. Where **E-1:** Fermenter; **E-2:** Decanter; **E-3:** Yeast Activation Tank; **E-4:** Absorption Column; **E-5:** Distillation Tower; **E-6:** Wastewater Treatment Plant; **E-7:** Decanter; **E-8:** Molecular Sieve; **E-9:** Evaporator.

The column's top sample has an ethanol concentration of 90.8 wt.% (Stream 14, Figure 1), approaching the azeotropic point of the ethanol/water mixture (95.64 wt.%). Additionally, the column-top stream has a concentration of higher alcohols (i.e., propanol, butanol, and pentanol) below 0.25 wt.%. These alcohols are fermentation by-products and are generally present in bioethanol obtained from sugarcane [29]. Concentrations for these higher alcohols were highest for the light medium, heavy medium, and bottom samples, which

reached values of 41.30, 1.79 and 1.31 wt.%, respectively (Streams 10, 12, and 13, Figure 1). The presence of higher alcohols is of special interest due to the susceptibility of the acid sites of the catalyst to interact with these compounds during ethanol dehydration. Hence, decomposition of higher alcohols with temperature results in unwanted by-products that could affect catalytic performance (i.e., acetaldehyde, propylene, and other aromatics) [22].

2.2. Catalyst synthesis

ZSM-5 zeolites (ACS material®, USA) with Si/Al ratio of 371, 280, and 26 were used; the H-ZSM-5 form was obtained by heating 1 g zeolite at 1 °C min^{-1} to 550 °C for 10 h in inert atmosphere using a 100 mL min^{-1} He stream. In addition, some zeolite samples were doped with Ce and Cu using the ion exchange method proposed by Di Iorio et. al. [30]. Briefly, H-ZSM-5 zeolite (1 g of zeolite per 100 mL of aqueous solution) was added to an analytical grade 0.1 M aqueous solution of $Ce(NO_3)_3 \cdot 6H_2O$ (Aldrich, USA) or analytical grade $Cu(NO_3)_2 \cdot 3H_2O$ (Aldrich, USA), adjusting to a pH of 5 with a 0.1 M NH_4OH solution. Subsequently, the solution was stirred at 300 rpm for 24 h at room temperature, dried for 24 h at 100 °C in a flask, and calcined at 550 °C for 4 h, using a ramp of 1 °C min^{-1}. The resulting catalysts were named "M-ZR" on the form, where M indicates the metal used as dopant and R the Si/Al ratio. Cu and Ce loadings were 0.3 and 0.1 wt.%, respectively, which was measured by Inductively coupled plasma mass spectrometry (ICP-MS).

2.3. Catalytic activity

The evaluation of the catalytic activity was carried out at an atmospheric pressure in a vertical quartz reactor (internal diameter of 16 mm) covered by a heating furnace (Applied Test Systems, USA) with a temperature control system. Quartz wool was used on top of the catalytic bed to generate turbulence in the reaction stream before reaching the catalyst. In all experiments, 50 mg of catalyst mixed with 50 mg of crushed quartz (particle size

between 0.18-0.12 mm) was used. Prior to the reaction, the catalyst samples were activated in N_2 atmosphere for 4 h at 550 °C with a ramp of 1 °C min^{-1}. A liquid flowrate of 0.034 mL min^{-1} of bioethanol was fed to the reactor using a Simdos 02 dosing pump (KNF Neuberger, USA). Before entering the reactor, the bioethanol was evaporated and mixed with N_2 (350 mL min^{-1}) as a carrier gas. Catalytic tests were performed under a WHSV of 30.2 h^{-1}, beginning the reaction at the maximum temperature of 400 °C and reducing the temperature each 50 °C until 200 °C. Additionally, some catalyst samples were subjected to stability tests at either 230 or 300 °C under a WHSV of 42.3 h^{-1}.

In all cases, the reactor outlet was connected to a condenser operating at 4 °C to collect unreacted ethanol and water. Non-condensable products were quantified by GC on a Clarus 580 (Perkin Elmer, USA), equipped with an HP-PLOT Q column (30 m x 0.53 mm x 40 µm, Agilent J&W) connected to a thermal conductivity detector (TCD), while a flame ionized detector (FID) was used for condensable products. The same procedure was followed for the stability tests, taking samples of the condensate every hour in triplicate in order to evaluate the conversion. The conversion of bioethanol, C_2H_4 selectivity, and WHSV were estimated according to the following equations:

$$Bioethanol\ conversion\ [\%] = \frac{n_B^{in} - n_B^{out}}{n_B^{in}} * 100 \quad (1)$$

$$C_2H_4\ Selectivity = \frac{n_{C_2H_4}}{n_B^{in} - n_B^{out}} * 100 \quad (2)$$

$$WHSV\ [h^{-1}] = \frac{F_B}{g_{cat}} \quad (3)$$

Where, n_{in}^B and n_{out}^B are the initial and final mol flowrate of bioethanol [mol/h], respectively. $n_{C_2H_4}$ is the outlet mol flowrate of ethylene [mol/h], g_{cat} is the mass of the catalyst and F_B is the mass flowrate of bioethanol [g/h].

2.4. Catalyst characterization

The catalyst acidity was measured by ammonia temperature-programmed desorption (NH_3-TPD) using a ChemBET Pulsar unit (Quantachrome Instruments, Boynton Beach, FL, USA) equipped with a TCD. Prior to the analysis, 0.1 ± 0.01 g of sample was activated in N_2 atmosphere for 4 h at 550 °C with a ramp of 1 °C min^{-1} after being degassed with N_2 (50 mL min^{-1}) at 120 °C for 1 h. Then, the sample was cooled down to 80 °C for the NH_3 adsorption, which was carried out by passing 50 mL min^{-1} of 5 vol% NH_3/N_2 through the sample for 60 min. After saturation with ammonia, the catalyst was purged with N_2 at 50 mL min^{-1} for 1 h to eliminate physically adsorbed NH_3. TPD data were collected from 50 to 1000 °C in N_2 flow of 50 mL min^{-1} with a ramp of 10 °C min^{-1}.

The crystal structure of the zeolites was studied by XRD. Spectra were recorded at 2θ with a step size of 0.05°, a step time of 3 s, and the peak position deviation was ≤ 0.002°. The relative crystallinity percentage of the zeolites was determined by the sum of the area of the crystalline peaks over the total sum of peaks (crystalline + amorphous), taking the major peaks of (102), (301), (202), (321), (113), (501), (422), (313), (512), (532), (616), and (1000) [31,32].

The dehydration of ethanol on the catalytic surface of zeolite samples was studied by *in-situ* DRIFTS, using a Nicolet iS10 spectrometer (Thermo Scientific, USA) equipped with a DRK-3 Praying Mantis diffuse reflection accessory (Harrick, USA) with SeZn windows. Zeolites were pretreated in N_2 inert atmosphere (47 mL min^{-1}) from room temperature to 500 °C with a ramp of 5 °C min^{-1} and maintained at that temperature for 4 h. The tests were carried out at 300 °C with a constant flow of He (50 mL min^{-1}). In order to observe the adsorption mechanism, upon reaching the reaction temperature, a bioethanol stream (0.03 mL min^{-1}) was fed by a metering pump (Simdos 02, KNF Neuberger, USA) and mixed with

the He stream (50 mL min^{-1}) as a carrier for 1h. Then, in order to see the desorption rate of the intermediaries, the sample was purged for 1h with He flow (50 mL min^{-1}). Spectra measurements were carried out in a range of 4000 - 600 cm^{-1} with an average of 32 scans and a resolution of 4 cm^{-1}. Each spectrum was obtained by subtracting the blank collected for the zeolite at the reaction temperature. Before starting the desorption, a blank of the zeolite with the adsorbed bioethanol was taken.

All raw and processed Excel data from catalytic activity and catalyst characterization results can be downloaded from [dataset] [33].

3. Results and discussion

3.1. Effect of the crude bioethanol impurities on the activity and selectivity of H-ZSM-5 during the ethanol dehydration to ethylene

In order to evaluate the crude bioethanol samples, catalytic dehydration using a zeolite Z280 at 300 °C was performed, since this catalyst showed better performance for synthetic bioethanol in previous studies carried out in our laboratory [17]. The ethanol conversion and selectivity to C_2H_4 obtained for the different bioethanol samples are shown in Figure 2. It is observed that higher ethanol concentration leads to a higher activity. For example, the top sample, which has a concentration of 90.82 wt.%, an ethanol conversion of 95% was achieved at 300 °C. Meanwhile, other samples with lower ethanol concentration require a higher temperature to obtain the same conversion. Moreover, the same pattern was observed for the selectivity to C_2H_4, which is higher in the ethanol-rich samples obtained from the distillation column (Figure 2b). Accordingly, the bioethanol sample of the top reached a 96% selectivity to C_2H_4 at 300 °C. Therefore, the presence of water is negatively affecting the reaction behavior, likely due to: (i) the fact that water is one of the reaction products, so its accumulation is affecting the equilibrium conversion in the ethanol

dehydration reaction [34] and (ii) the active sites of the catalyst can competitively adsorb it [35], decreasing the probability of ethanol interaction with the catalyst to form C_2H_4. This agrees with previously reported by Yao et al. [36], who proposed to carry out the process with bioethanol samples with concentrations > 75 vol% (70.3 wt.%) to achieve selectivity above 95%. Thus, the other fractions (i.e., light medium (12.43 wt.%), heavy medium (10.78 wt.%), and bottom (7.76 wt.%)) can lead to a drastic reduction of the activity and the selectivity of the process.

However, not only water is affecting the catalyst behavior. For instance, the light medium fraction showed an ethylene selectivity as low as 19% at 400 °C (Figure 2b), which is probably due to its elevated concentration of isoamyl alcohol (41.3 wt.% of $C_5H_{12}O$ in Figure 1), a strong catalyst poison, as reported by Sanchez et al. [29] in bioethanol reforming reactions. Therefore, the presence of larger amounts of impurities requires additional rigorous purification steps. The following sections will focus on the results obtained using the distillate top fraction, a sample with elevated concentrations of ethanol and low amounts of impurities, but still a not-rigorous distillated sample, by evaluating different H-ZSM-5 zeolite-based catalysts.

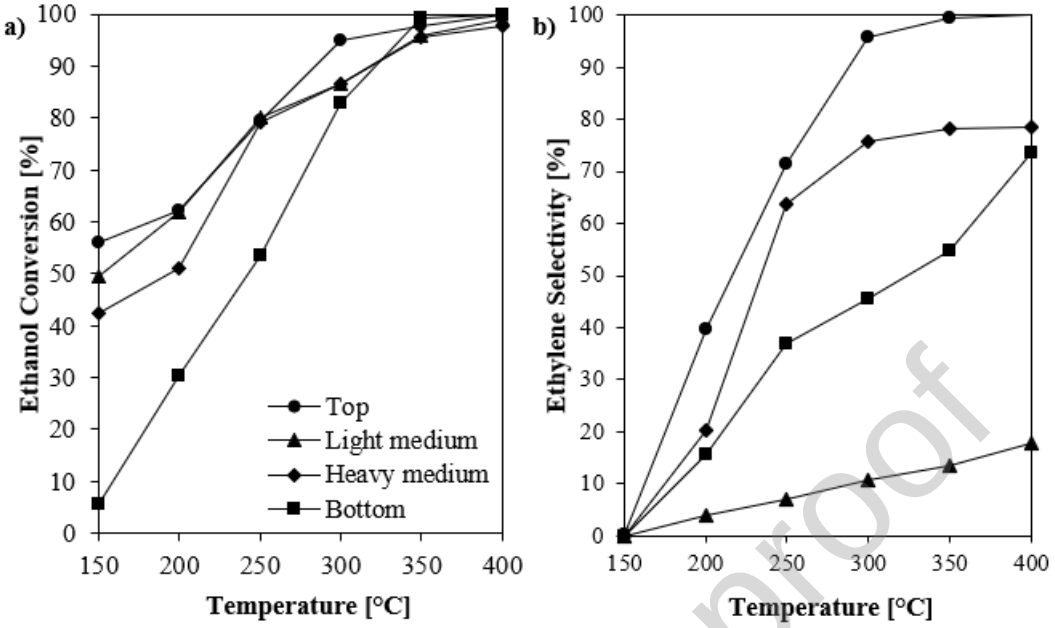

Figure 2. Catalytic activity of the different bioethanol samples using the zeolite Z280: **a)** Bioethanol conversion and **b)** Selectivity to C_2H_4 during bioethanol dehydration. Conditions: 50 mg catalyst, WHSV=28.4 h^{-1}. Refer to Figure 1 to check the bioethanol samples concentration.

3.2. Effect of the ZSM-5 Si/Al ratio and doping on the dehydration of the bioethanol top sample to ethylene

Figure 3 shows the conversion of ethanol and the selectivity to C_2H_4 during the catalytic dehydration of ethanol using the zeolites Z26 and Z371 doped with Ce and Cu using the bioethanol distillate top fraction. Z280 results were included for comparison due to Z26 showed better performance when these kind of crude bioethanol samples were dehydrated (see Figure 2). Figures 3a and b show the conversion of ethanol obtained with ZSM-5 zeolite-based catalysts. Zeolite Z26 showed the highest activity, reaching 97.47% ethanol conversion at 250 °C, while the other catalysts at the same temperature have activities below 80%. Doping negatively influences ethanol conversion (Figures 3a and b) and it is

more significant in the zeolite with lower Si/Al ratio (i.e., Z26). For example, at 250 °C (Figures 3a and b), the conversion on Cu- and Ce-doped samples of Z26-based catalysts decreases on average by 18%, while on Z371-based samples the activity the decrease in activity is 12%.

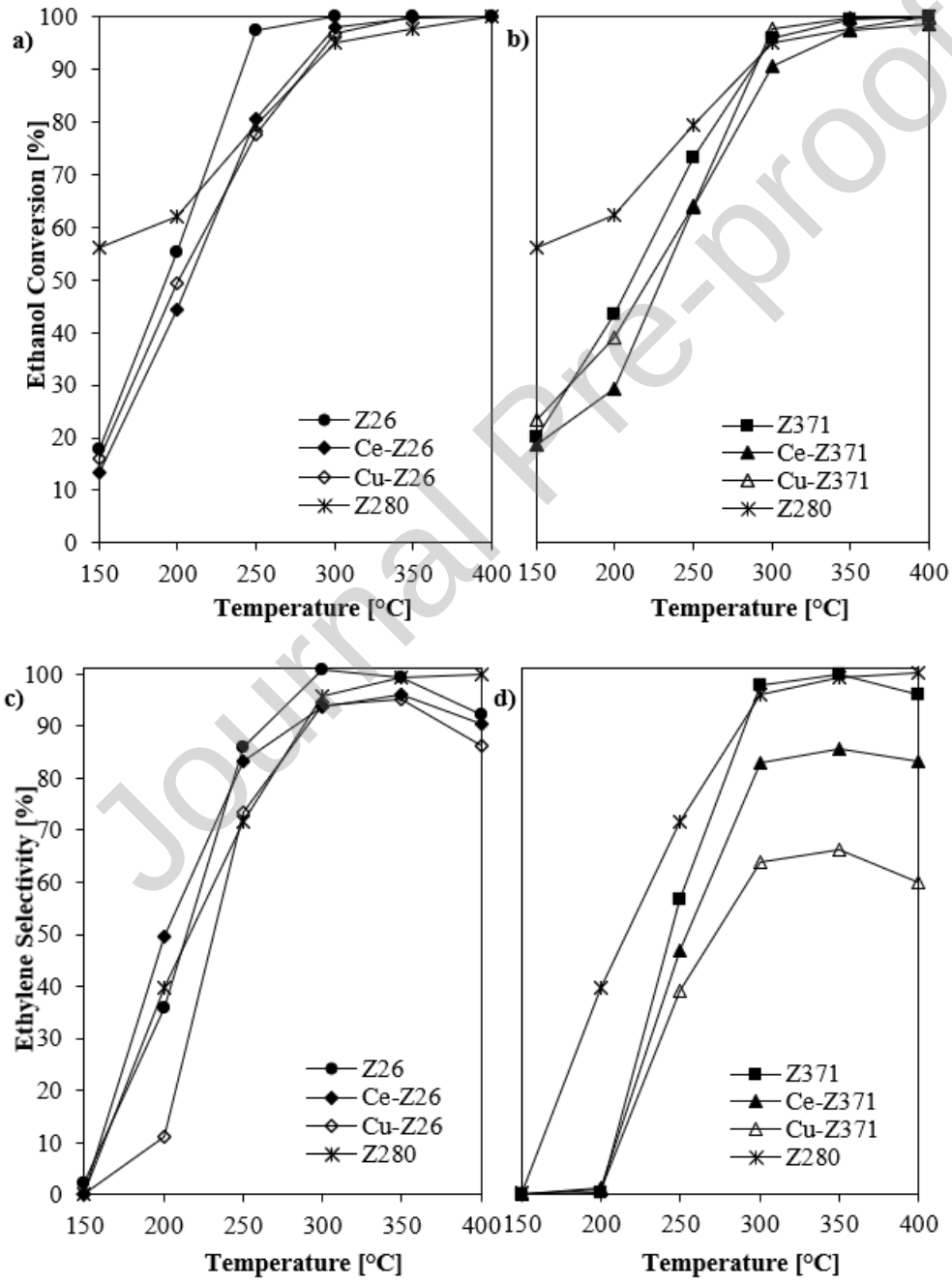

Figure 3. Catalytic activity of the different zeolite samples during bioethanol dehydration as a function of temperature **(a, b)** Bioethanol conversion and **(c, d)** selectivity to C_2H_4. Conditions: 50 mg catalyst, WHSV=30.2 h^{-1}, bioethanol top sample.

On the other hand, Figures 3c and d show the selectivity to C_2H_4 of the ZSM-5 based catalysts. Selectivity to C_2H_4 is also favored at lower Si/Al ratios. At 300 °C, where all catalysts achieve ethanol conversions above 90%, the selectivity decreases in order Z26 (100%) > Z280 = ZSM5-371 (96%) > Ce-Z26 = Cu-Z26 (94%) > Ce-Z371 (83%) > Cu-Z371 (64%). Thus, low Si/Al ratios simultaneously favor activity and selectivity in the dehydration of crude bioethanol over ZSM-5 zeolites. In a similar way to what was observed with the activity, the inclusion of Ce and Cu as dopants in the H-ZSM-5 zeolite has a negative effect on the selectivity to C_2H_4. However, the decrease in selectivity is more pronounced in samples with higher Si/Al ratios, reducing selectivity by up to 33% in the Cu-Z371 sample compared to its respective undoped zeolite (i.e., Z371).

In our earlier study on the pure ethanol dehydration to ethylene, we reported a complete ethanol conversion and ethylene selectivities of 70, 60, and 50% for ZSM5-23, ZSM5-30, and ZSM5-280 zeolites, respectively, at 300 °C and under a WHSV of 13.8 h^{-1} [17]. Since we are currently obtaining similar results, impurities (i.e., C_3H_8O, $C_4H_{10}O$, and $C_5H_{12}O$) present in the top fraction bioethanol sample used in this study (i.e., 90 wt.% ethanol) do not show a negative impact on the catalytic performance (see Figure 2). In fact, Banzaraktsaeva et al. [37] reported a conversion of 96% and selectivity to C_2H_4 of 97% for bioethanol samples (ethanol 92.5 wt.%) with an impurity concentration of 0.43 g L^{-1} using an Al_2O_3 catalyst at 400 °C, suggesting that an isopropanol concentration of up to 0.7 g L^{-1} benefits dehydration, as it decreases the amount of generated by-products [37]. Thus, the catalyst performance in the dehydration of top fraction of crude bioethanol would depend

mainly on the Si/Al ratio and dopants. Contrary to that reported in [19,38], doping ZSM-5 zeolites lead to less active catalysts in the dehydration of ethanol to produce ethylene and several authors have reported different reasons related to textural changes in the catalyst [39,40]. To study this effect, the catalyst samples were characterized by several techniques, which are discussed in the following section.

3.3. Catalyst characterization

3.3.1. XRD

Figure 4 shows the XRD spectra of the ZSM-5 zeolite-based catalysts. All samples have well-defined 2θ spectra with characteristic high-intensity Bragg peaks between 22 and 25°, indicating that the ZSM-5 zeolite used has a crystalline structure [31]. However, Ce and Cu peaks were not detected in XRD spectra probably by their low concentration (< 0.5 wt.% by ICP-MS) [41].

The relative crystallinity of samples measured with XRD decreases in order Z280 (81.9%) > Z371 (78.8%) > Z26 (78.6%) > Ce-Z26 (76.5%) > Ce-Z371 (76.2%) > Cu-Z371 (72.5%) > Cu-Z26 (71.0%). This trend is similar to that observed for activity and selectivity to C_2H_4 (Figure 3), where the presence of dopants (i.e., Cu and Ce) decrease catalyst performance. Triantafyllidis et al. [31] suggest that even slight differences in relative crystallinity would lead to significant changes in catalytic performance during isopropanol dehydration over ZSM-5 zeolites. Thus, the inclusion of dopants in the zeolite crystal lattice leads to lower crystallinity and thus lower selectivity. The change in the crystalline structure of zeolites due to the presence of metals could also alter the acidity and the capacity of the zeolite to interact with crude bioethanol and form intermediaries. Therefore, the ZSM-5 zeolite samples were evaluated by NH_3-TPD and *in-situ* DRIFTS, as follows.

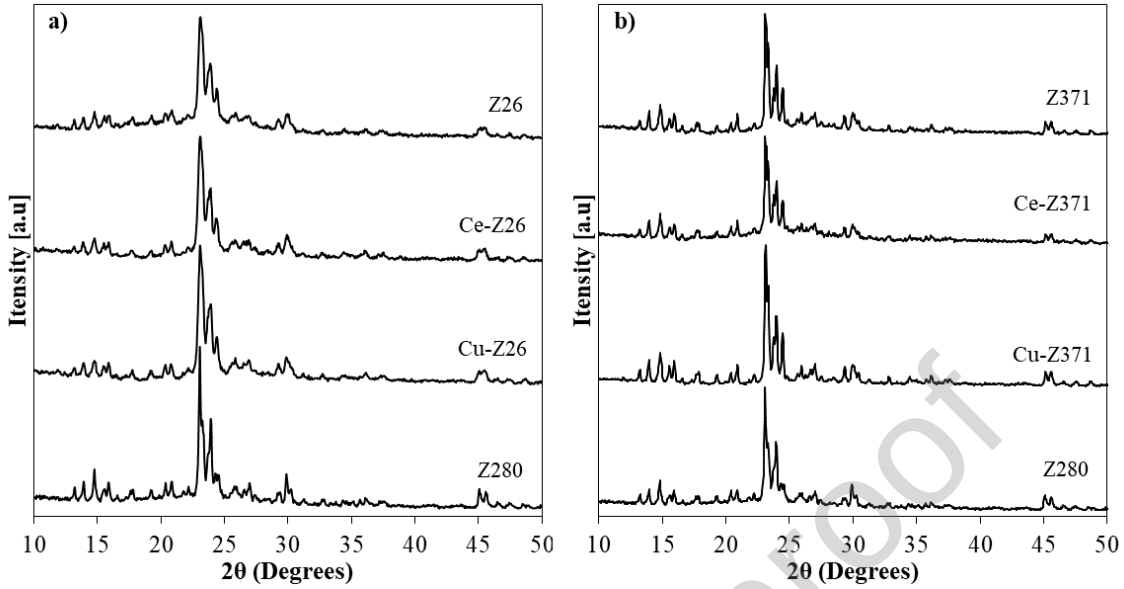

Figure 4. XRD spectra of zeolites **a)** Z26, Ce-Z26, and Cu-Z26, and **b)** Z371, Ce-Z371 and Cu-Z371. The Z280 samples are included for comparison.

3.3.2. Temperature-programmed desorption of NH_3

NH_3-TPD is a useful technique to determine the surface acidity of solid acid catalysts. The accuracy of this technique has been validated and is well-established [42,43]. Therefore, Figure 5 presents the desorption peaks and acid strength of Z26 and Z371 doped with Ce and Cu, while Table 1 provides a summary of the acid amount of the catalysts. Z280 results were included for comparison. As expected, zeolites with a lower Si/Al ratio exhibit a greater abundance of acid sites [8]. Z26 and Z280 samples exhibit three distinct desorption peaks, with the first occurring within the 80-150 °C range, related to weak acidity. The subsequent peaks, observed between 150-400 °C, are attributed to moderate and strong acid sites [42]. In contrast, Z371 samples display only weak and moderate acidity peaks. The catalytic activity of zeolites depends on the synergy between crystallinity and acidity [44]. Despite the fact that Z26 has a lower crystallinity than Z371 and Z280 (see Section 3.3.1), its superior acidity enhances catalytic performance in bioethanol dehydration (see Table 1).

Indeed, while a high crystallinity typically improves acid site accessibility, the higher amount of acid sites in Z26 (1.34 NH_3 mmol/g_{cat}) ensures effective reactant-acid site interactions, showing the crucial role of acidity in catalytic efficiency and allowing Z26 to improve activity and selectivity.

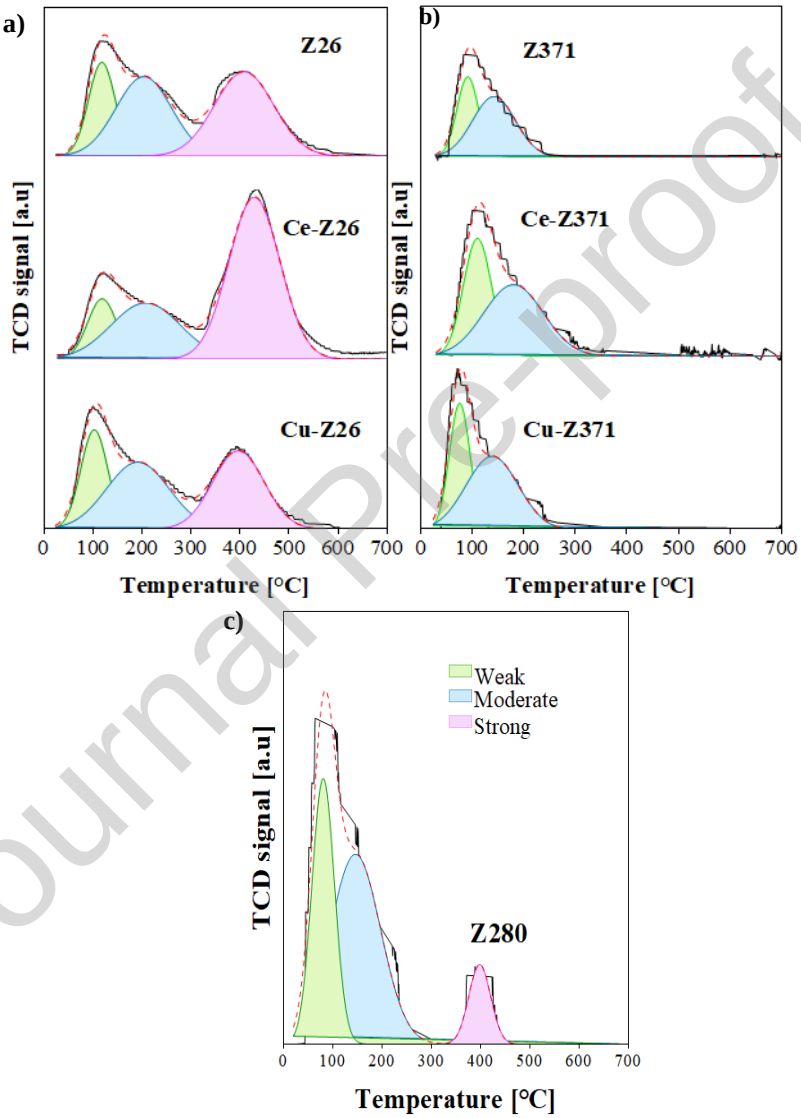

Figure 5. NH_3-TPD profiles for the different zeolite samples: (a) Z26, (b) Z371, and (c) Z280. Red line is the total fit of experimental data (black).

Doping has a significant impact on the acidity of the catalysts. Specifically, Ce^{+3} ion exchange has a pronounced effect, altering the distribution and density of acid sites, mainly

within Z26 compared to Z371 (Figure 5). The introduction of Ce ions via ion exchange potentially enhances the Lewis and Brønsted acid character of the Ce ions in contrast to Al ions [45]. This exchange also enhances the zeolite's ability to interact with molecules possessing electron pairs, thereby increasing the abundance of both acid sites. As a result, Ce-Z26 had the largest acidity among the studied zeolites. The difference between Z26 and Z371 is most likely due to the larger quantity of Al atoms in Z26, which results in a less dense zeolitic structure and a greater number of Si-OH-Al Brønsted acid sites available for exchange with Ce^{+3}. Moreover, further research suggests that rare earth oxide loading can drastically affect the distribution of strong and weak acid sites [46]. In contrast, doping with Cu^{+3} did not affect total acidity, but changed the distribution of the acid sites, causing them to move at a lower temperature in the case of Z26 and at a higher temperature in the case of Z371.

Therefore, the moderate and strong acid strengths increase in the doped catalysts can be related to their reduction in activity and stability during bioethanol dehydration, as shown in Figure 3. These findings align with results from Sun et al. [46], who reported an increase in acid strength (from 0.0119 to 0.135 mmol NH_3/g_{cat}) upon introducing Ce into ZSM-5 (Si/Al=25) catalysts. The inclusion of cations in H-ZSM-5 leads to interactions with H+ species on the zeolite surface, thereby altering the distribution of acid sites and selectivity [45]. Also, Brønsted acid sites favors olefin polymerization and the formation of carbonaceous compounds [19], which tend to diminish the catalyst activity and selectivity. The relationship between acid sites and selectivity in ethanol dehydration remains a topic of debate. In the current study, which utilized crude bioethanol as a feedstock, the inclusion of dopants such as Ce and Cu resulted in an increased density of strong acid sites, which harmed the catalytic performance of the ZSM-5 zeolites, affecting both their activity and

selectivity. Nevertheless, the influence of these dopants on the stability of H-ZSM-5 zeolite will be investigated further in the catalyst stability section.

Table 1. Amount of NH_3 desorbed over different zeolite samples.

Catalyst sample	Weak		Moderate		Strong		Total acid amount [mmol NH_3/g_{cat}]
	T [°C]	mmol NH_3/g_{cat}	T [°C]	mmol NH_3/g_{cat}	T [°C]	mmol NH_3/g_{cat}	
Z26	119	0.28	204	0.50	409	0.56	1.34
Ce-Z26	119	0.25	209	0.57	431	1.20	2.02
Cu-Z26	103	0.30	192	0.47	397	0.45	1.22
Z280	81	0.05	146	0.07	398	0.01	0.13
Z371	92	0.07	143	0.11	-	-	0.18
Ce-Z371	110	0.09	181	0.12	-	-	0.21
Cu-Z371	110	0.09	181	0.12			0.21

3.3.3. DRIFTS of ethanol dehydration on different zeolites

Figure 6 shows the DRIFTS for H-ZSM-5 zeolites at different Si/Al ratios during adsorption of bioethanol followed by purging in an inert atmosphere. For all zeolites, changes were observed in 3 main zones of the spectra; Lewis acid sites found at 3738 cm^{-1} (e.g., Si─OH), which correspond to the first zone (I in Figure 6), activate ethanol through coordination with oxygen and water [8]. Also, the bands found at 3500 and 3670 cm^{-1} are associated with Brønsted acid sites formed by OH- groups attached to Al in the outer and inner framework of zeolites, respectively (i.e. Si─OH─Al). Brønsted acid sites facilitate the protonation of the hydroxyl group bridging CO species in ethanol, allowing ethanol dehydration [8,19]. The second zone (II in Figure 6) corresponds to the region of symmetric and asymmetric vibrations of the ─CH_3 and ─CH_2 groups of the ethoxy groups formed by the adsorption of ethanol (2982 and 2934 cm^{-1}); and the third zone (III in Figure 6) between 1200 and 1900 cm^{-1} corresponding to the formate and carbonate groups adsorbed on the catalyst surface (C─O groups). Additionally, for all three zeolites, a band at 2345 cm^{-1}

corresponding to the molecular gas phase of CO_2 was observed and the formation of water as a reaction product in the band at ~1330 cm^{-1} [17] was also evidenced.

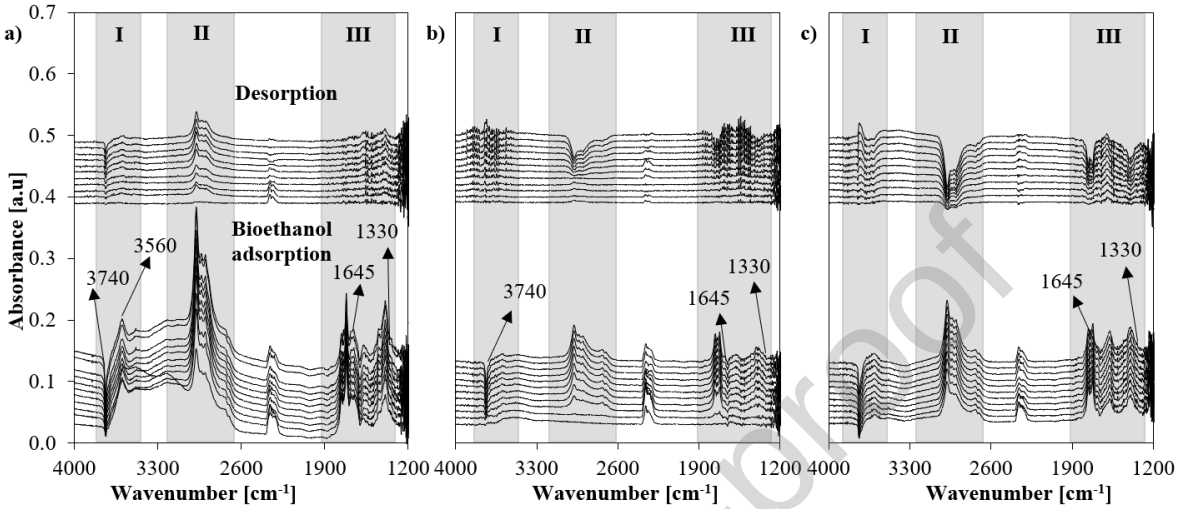

Figure 6. *in-situ* DRIFTS during bioethanol dehydration of zeolite **a)** Z26, **b)** Z280, **c)** Z371 at 300°C.

In Zone I, during the adsorption step, a negative band was observed in the region of 3745 - 3620 cm^{-1} along with a negative band centered at ~3740 cm^{-1} corresponding to the adsorption of bioethanol on the OH^- groups of the zeolite [17,47]. In addition, it was observed that a new band ~3560 cm^{-1} is formed, which corresponds to vibration of the ─OH of the adsorbed bioethanol [47], being more intense for the Z26. At lower Si/Al ratios, the capacity to adsorb ethanol increases in H-ZSM-5 zeolites due to their greater amount of acid sites (see Section 3.3.2), which may be related to the higher activity of Z26 (Figure 3). On the other hand, during desorption (purging), the bands associated with ethanol adsorbed on zeolites gradually disappear; desorption occurs rapidly in samples Z280 and Z371. Therefore, although higher Si/Al ratios in H-ZSM-5 increases their relative crystallinity, i.e., more ordered structures, the adsorption capacity is directly related to the amount and strength of the acid sites, leading to a lower activity over Z280 and Z371.

In Zone II (Figure 6) associated with the formation of ─CH_3 and ─CH_2 groups, a higher intensity (2900─2600 cm^{-1} region) is observed for the zeolite with a lower Si/Al ratio (i.e., Z26, Figure 6a) than for zeolites with a higher Si/Al ratio (Z280 and Z371 in Figures 5b and c, respectively) [48]. The above suggests that, in addition to facilitating ethanol adsorption, zeolite Z26 promotes the formation of C_2H_4, which is confirmed by the bands at ~2880 and ~1645 cm^{-1} [49]. However, desorption of ethoxy groups is slower in zeolite Z26 (Figure 6a), suggesting that product desorption could be the limiting step in the catalytic cycle of zeolites with a lower Si/Al ratio.

The presence of adsorbed formate and carbonate groups [48] (Zone III in Figure 6) also changes at different Si/Al ratios in H-ZSM-5 zeolites. In comparison with the previously reported synthetic ethanol adsorption DRIFTS [17], these results show the presence of additional bands at 1446 and 1557 cm^{-1}, which would be associated with symmetric and asymmetric vibrations of intermediaries such as acetates (O─C─O) [50], respectively, favored by the presence of impurities in the crude bioethanol.

In general, zeolite Z26 favors higher formate and carbonate formation over Si─O─Al groups (1250 cm^{-1}) [50,51], these are intermediaries in the dehydration of ethanol to form olefins such as C_2H_4 [52], which explains its higher activity compared to H-ZSM-5 samples with higher Si/Al ratios. However, the presence of Brønsted acid sites favors not only the ethanol dehydration but also the olefin polymerization and the formation of carbonaceous compounds and aromatic deposits [17], including the 1645 cm^{-1} peak corresponding to the C=C group [49]. Also, during desorption, the Z26 catalyst appears to form strong bonds with formates and carbonates as it releases them more slowly compared to the other undoped samples (i.e., Z280 and Z371).

Figure 7 shows the DRIFTS of ZSM-5 zeolites doped with Ce (Figure 7 a, b) and Cu (Figure 7 c, d), retaining the same analysis zones previously described for Figure 6. In Zone I, it is observed that, in the samples doped with Ce (Figure 7 a and b), the adsorption capacity of bioethanol decreases in comparison with their respective samples without doping (i.e., Z26 and Z371 in Figure 6). This agrees with the activity results (Figure 3), where the presence of dopants decreases the conversion of crude bioethanol. Cu doping (Figure 7 c and d) has an even more pronounced negative impact on the adsorption capacity of ethanol, especially in the Cu-doped ZSM-5 sample (Figure 7c). However, in Zone I, the band associated with the OH group and the Brønsted acid sites (~3740) is regenerated by rapid desorption, which allows accessibility to new ethanol molecules [53]. This effect is more visible in Ce-Z26 due to its higher density of strong acid sites (see Table 1). Furthermore, in Zone II it is observed that the dopant also influences the formation of ethoxy species involved in the formation of C_2H_4 [49]. Both dopants (i.e., Ce and Cu) show less intense bands in the 2900─2600 cm^{-1} region compared to the undoped samples (Figure 6), which would be associated with their lower selectivity to C_2H_4 (Figure 3). However, the most interesting observation is that both dopants (Ce and Cu) favor a higher desorption capacity of ethoxy groups. That is, although doping reduces the ability of the catalyst to form ─CH_3 and ─CH_2 groups, impacting selectivity (Figure 3), it also appears to favor product desorption, which would have relevance over long periods of operation (as will be discussed below). Finally, the presence of adsorbed formate and carbonate groups, and the band at ~1330 cm^{-1} associated with water, also decrease with doping (Zone III in Figure 7) compared to undoped samples (Zone III in Figure 7), which would be in line with the lower selectivity of the doped catalysts. The same is also observed in the intensity of the 1446 and 1557 cm^{-1} bands (possibly OCO groups [50]) which we assume are formed from impurities

present in the crude bioethanol. However, as observed in Zone III, Ce- and Cu-doped catalysts appear to be more effective in the desorption of formats, carbonates, and water that can form occlusions in the active sites of the catalyst, leading to the formation of carbon deposits [53]. Intermediaries desorption could have a greater impact on Ce-Z26 for longer reaction times since more acid sites would be available faster to adsorb new bioethanol molecules, as seen in the NH_3-TPD results.

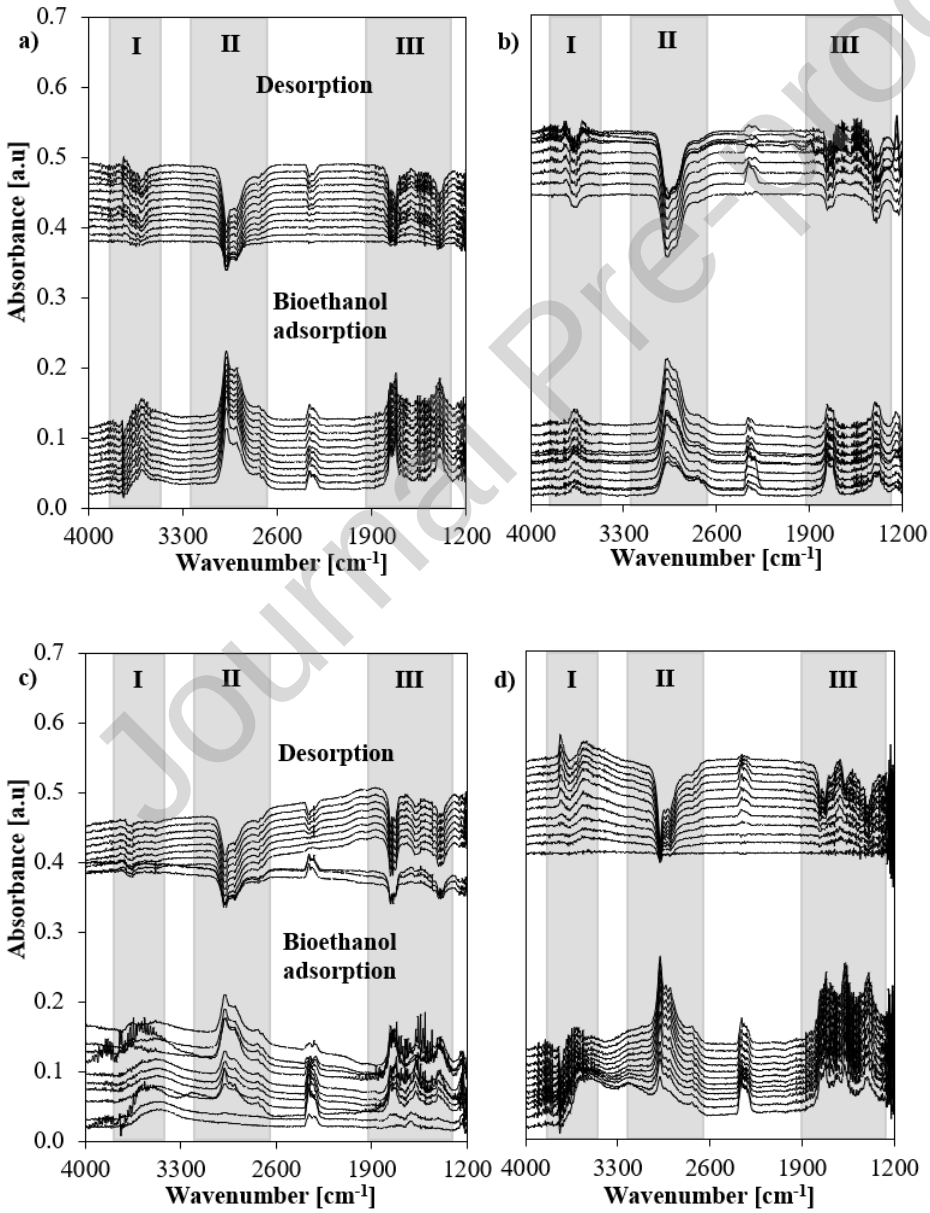

Figure 7. *in-situ* DRIFTS during bioethanol dehydration of zeolite **a)** Ce-Z26, **b)** Ce-Z371, **c)** Cu-Z26, and **d)** Cu-Z371 at 300°C.

Therefore, Z26 showed an enhanced capacity to adsorb ethanol during the dehydration of crude bioethanol due to a large availability of acid sites and a high relative crystallinity. In this context, a great variety of intermediaries can be formed on the catalytic surface, explaining the Z26 higher activity and selectivity. However, its deficiency in desorbing the reaction intermediaries can be a drawback during long periods of operation. This deficiency might be mitigated by the presence of dopants since they increase amount of acid sites (Section 3.3.1). Then, the stability of the Z26 zeolite and the most active doped catalyst (i.e., Ce-Z26) is addressed in the following section.

3.4. Catalytic stability

Previous sections showed us that lower Si/Al ratios increase the ethanol adsorption capacity of the ZSM-5-based zeolites during the crude bioethanol dehydration probably due to their larger acidity. This is in agreement with that reported by Le Van Mao et al. [54], who recommended Si/Al ratios between 35 to 55 to optimize synthetic bioethanol conversion and ethylene production. However, the inclusion of dopants such as Ce and Cu impacted negatively on the catalytic performance during the dehydration of crude bioethanol, which is opposite to that reported by other authors. For example, zeolites doped with Fe [19], La [18], and Cu [27] have shown improved olefin production from synthetic bioethanol compared to their undoped counterpart because doping with these metals results in an alteration in catalyst acidity [45]. However, there are no reports in the literature of the use of Ce as a dopant of ZSM-5 zeolites for ethanol dehydration. On the other hand, DRIFTS tests show that, despite its higher activity and selectivity, the deficiency to desorb the

reaction products could be a limiting factor in the use of Z26 in prolonged processes. Also, Ce was the dopant that increased the most the catalytic activity (Figure 3), due to an augment of the strong acid sites density on the catalyst surface (see section 3.3.2), and showing a higher bioethanol adsorption capacity (see section 3.3.3). Therefore, this section presents the results of several stability tests over Z26 and Ce-Z26, increasing the WHSV from 30.2 to 42.3 h^{-1} and under two different reaction temperatures (i.e., 230 and 300 °C). Figure 8 shows that the two samples (i.e., Z26 and Ce-Z26) maintain full conversion of crude bioethanol during 140 h TOS at 300 °C. Similar results have been reported by Masih et al. [55] for a H-ZSM-5 with a Si/Al of 23.3 at 300 °C and Wu et al. [24] for zeolites P/ZSM-5-280 and La/ZSM-5-280 at 240 °C. Additionally, Z26 (Figure 8a) maintained a selectivity to C_2H_4 of 68% at 300 °C, while the Ce-doped sample (Figure 8b) showed a progressive increase until reaching a selectivity to C_2H_4 of 76% at the end of the test at 140 h.

Variation in selectivity during ethanol dehydration has been reported in several studies [18,55,56]. Hence, the inset plots depicted in Figure 8 provide an insightful analysis of the activity and selectivity of Z26 and Ce-Z26 samples at 230 °C. This experimental approach intends to study any potential catalyst deactivation under more strict conditions (i.e., stability at lower conversion). However, no conclusive proof of considerable deactivation was found for either of the catalysts in this conversion regime. Indeed, the Ce-doped sample showed a slight improvement in conversion at 35 h. However, the most significant changes occurred in selectivity. Notably, the undoped sample (Z26) had a dramatic reduction in ethylene selectivity, decreasing from 60% to 15% over the 55 h TOS. These findings highlight the critical role of Ce as dopant in C_2H_4 selectivity, making Ce-Z26 a significantly more stable catalyst than unmodified Z26. This improvement in stability is

mostly due to the reduction of carbon deposits on the catalytic surface, which is typically associated with zeolite type catalysts [57].

Accordingly, TGA results of fresh and used samples show that the Z26 zeolite present 47% more carbon deposits after 140 h TOS compared to the Ce-Z26 doped sample. Also, the increased acidity in this sample, due to the presence of Ce, would mitigate the coke formation since strong acid sites avoids carbonization of intermediaries [57]. In addition, Ce also contributes to decrease the formation of C-C chains [58]. Thus, doping Z26 with Ce leads to a zeolite with higher acidity (section 3.3.2) and lower ethanol adsorption capacity. However, it also favors a higher desorption of reaction intermediaries and a lower formation of carbonaceous compounds, improving the selectivity to C_2H_4 in continuous operation, as expounded in the DRIFTS section (3.3.3), in conjunction with its abundant acid content (Table 1). This characteristic is important for scaling up C_2H_4 production from crude bioethanol, where selectivity could play an even more important role than the activity.

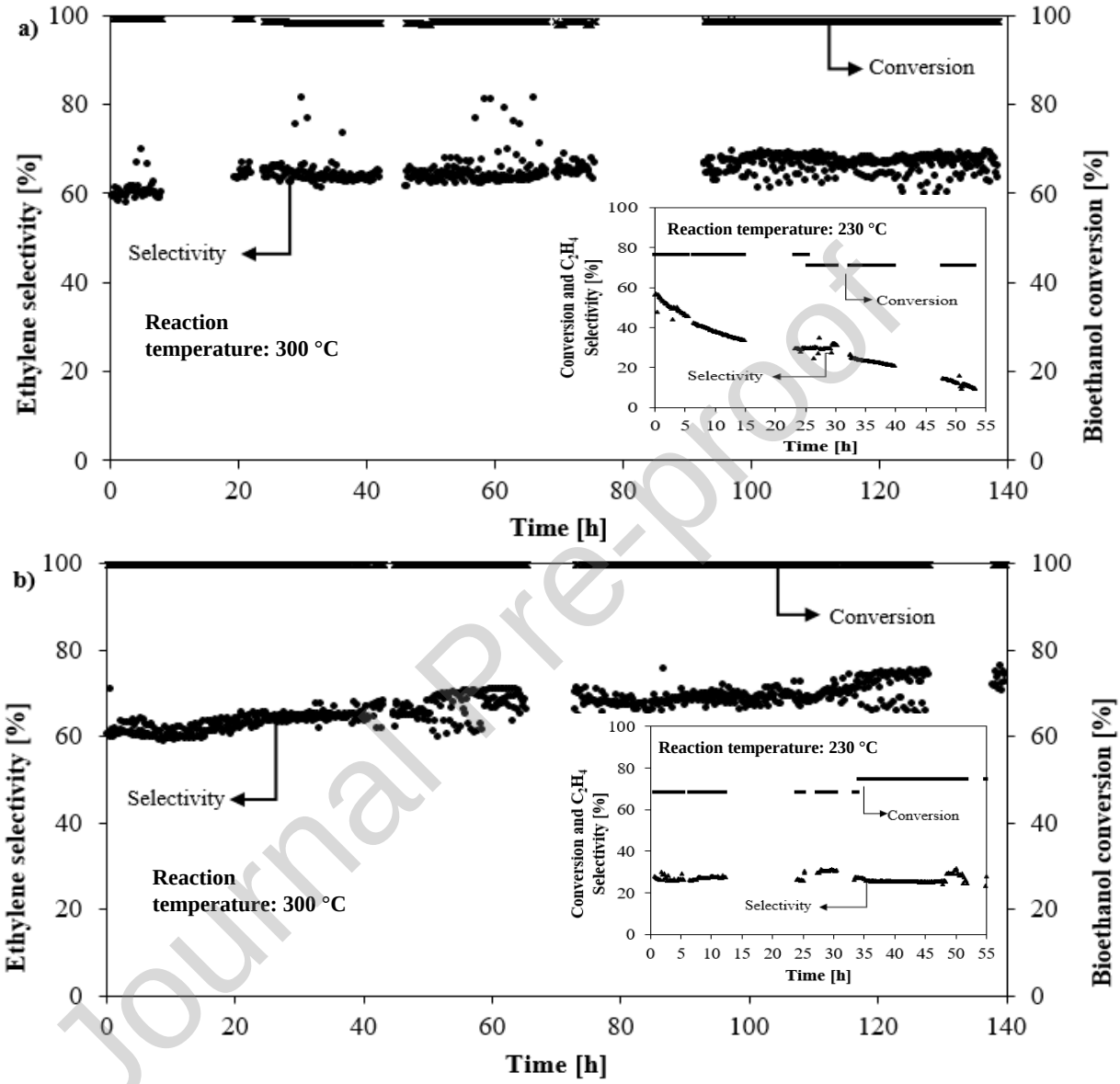

Figure 8. Conversion and selectivity of bioethanol dehydration (top) during a zeolite stability test **a)** Z26. **b)** Ce-Z26. Conditions: 50 mg catalyst, 300°C, WHSV=42.3 h^{-1}, bioethanol top sample. The inset plots show the stability test at 230 °C.

Table 2 compares the results of this study with other reports in the literature, where ZSM-5 zeolites with different doping and Si/Al ratios were used. The bioethanol conversion in all cases is greater than 90%, confirming the effectiveness of this type of zeolites in ethanol

dehydration. However, most studies focus on synthetic bioethanol samples (90-60 wt.% ethanol samples in water). Thus, contributions with results where crude bioethanol dehydration is evaluated could be an important advance in establishing this technology in the future. In this study, conversions higher than 98% and stability during 140 h TOS were obtained using unpurified sugarcane bioethanol.

Table 2. Comparison of bioethanol to ethylene dehydration studies

Bioethanol type	**T [° C]**	**Impurities**	**Catalyst**	**WHSV [h^{-1}]**	**Catalyst [g]**	**Scale**	**Conv. [%]**	**S [%]**	**Stability [h]**	**Ref**
Synthetic 90 wt.%	250	None	ZSM5-23	2	0.5	Lab	100	93	20	[18]
Synthetic 90 wt.%	260	None	La-ZSM5-23	2	12	Bench	90	85	95	[18]
Synthetic 90 wt.%	260	None	ZSM5-23	2	12	Bench	90	73	300	[18]
Synthetic 60 wt.%	260	None	Fe-ZSM5-25	0.81	3	Lab	98	97	1440	[19]
Synthetic 60 wt.%	260	None	ZSM5-25	0.81	3	Lab	96.8	70	70	[19]
Raw 99 wt.% From sugarcane	280	None	Ti-ZSM5-20	7	1	Lab	96	88	-	[20]
Raw 92.5 wt.% From miscanthus	400	Alcohols and esthers	53 %γ-Al_2O_3 and 47 % χ-Al_2O_3	-	2.87	Lab	96	97	-	[37]
Raw94 wt.% From Oat hulls	400	Alcohols, aldehydes and esthers	Al_2O_3	-	2.87	Lab	83-91	94	-	[59]
Raw 90.82 wt.% From sugarcane	300	Alcohols	Z26	42.3	0.05	Lab	99	65	140	This work
Raw 90.82 wt.% From sugarcane	300	Alcohols	Ce-Z26	42.3	0.05	Lab	99	67	140	This work

On the other hand, previous studies have been performed at low WSHV (< 7 h^{-1}) compared to this study, where catalysts were evaluated at WSHV above 30 h^{-1} which entails a condition closer to extensive processes. Chen et al. [19] found that, with increasing WHSV, the selectivity to C_2H_4 decreases due to a shorter contact time of ethanol molecules with the catalyst, leading to the formation of DEE [19]. In our case, we observed similar results where the increase in WHSV from 30.2 to 42.3 h^{-1} between the activity test and the stability test reduced the selectivity of sample Z26 by 32%. Despite this, it was observed that, in prolonged processes, the stability of Ce-doped Z26 could increase the stability in the selectivity to ethylene with a WHSV of 42.3 h^{-1} by up to 26% because this new catalyst favors product desorption during the catalytic cycle and mitigates the formation of carbonaceous compounds.

Conclusions

The dehydration of crude bioethanol over H-ZSM-5 zeolites as catalysts to produce C_2H_4 was studied. It was observed that, at higher ethanol concentrations (90.82 wt.%), the highest conversion (95%) and selectivity to C_2H_4 (96%) were obtained with Z280 at 300 °C and WHSV of 28.4 h^{-1}. However, when varying the Si/Al ratio, lower ratios increase the activity due to the higher concentration of acid sites (>1.2 mmol NH_3/g_{cat}) and higher crystallinity observed by XRD.

In-situ DRIFTS studies show that, among the tested zeolites and reaction conditions, bioethanol adsorbs preferentially on acid sites of HZSM-5 with a Si/Al ratio of 26 at 300 °C, leading to the formation of ethoxy C─O species attached to OH groups of the zeolite, generating C_2H_4, and releasing water as a by-product. In addition, the desorption of ethoxy

groups and other intermediaries is favored by the presence of dopants such as Ce, which favors the stability of the catalyst, avoiding their deactivation in prolonged periods of operation.

Doping ZSM-5 zeolites with Ce favors higher desorption of reaction intermediaries, increase the total acidic sites, and reduce the formation of carbonaceous compounds, which led to a progressive increase in selectivity to C_2H_4 during 140 h TOS. Also, it prevents deactivation in under more drastic conditions for a 50 h TOS compared with a undoped zeolite.

Acknowledgments

The authors thank the Universidad de La Sabana for funding through the ING-212-2018 project and the International Relations Department of the University of Alicante (program named "University Development Cooperation 2020") for their financial support for the NH_3-TPD analysis performed in this work.

Contributions

Eliana Quiroga: Methodology, Validation, Formal analysis, Research, Data processing, Original drafting-writing, Visualization **Nicolas García:** Validation, Formal analysis, Research, Data processing, Original drafting-writing, Visualization **Bernay Cifuentes:** Formal Analysis, Data Processing, Writing-Original Drafting, Writing-Revision and Editing, Visualization **Ricardo Cogua:** Methodology, Research, Data processing **Jorge Becerra:** Formal Analysis, Writing-Revision and Editing **Julia Moltó:** Resources, Supervision, Research, Data processing, Fund Acquisition **Martha Cobo:**

Conceptualization, Methodology, Formal Analysis, Resources, Writing-Revision and Editing, Supervision, Project Management, Fund Acquisition.

References

[1] L.L.N. Guarieiro, J.P. dos Anjos, L.A. da Silva, A.Á.B. Santos, E.E.S. Calixto, F.L.P. Pessoa, J.L.G. de Almeida, M. Andrade Filho, F.S. Marinho, G.O. da Rocha, J.B. de Andrade, Technological Perspectives and Economic Aspects of Green Hydrogen in the Energetic Transition: Challenges for Chemistry, J. Braz. Chem. Soc. 33 (2022) 844–869. https://doi.org/10.21577/0103-5053.20220052.

[2] F. Jamil, M. Aslam, A.H. Al-Muhtaseb, A. Bokhari, S. Rafiq, Z. Khan, A. Inayat, A. Ahmed, S. Hossain, M.S. Khurram, M.S. Abu Bakar, Greener and sustainable production of bioethylene from bioethanol: current status, opportunities and perspectives, Rev. Chem. Eng. 38 (2022) 185–207. https://doi.org/10.1515/revce-2019-0026.

[3] J.B. Heo, Y.S. Lee, C.H. Chung, Raw plant-based biorefinery: A new paradigm shift towards biotechnological approach to sustainable manufacturing of HMF, Biotechnol. Adv. 37 (2019) 107422. https://doi.org/10.1016/j.biotechadv.2019.107422.

[4] I. Rossetti, A. Tripodi, G. Ramis, Hydrogen, ethylene and power production from bioethanol: Ready for the renewable market?, Int. J. Hydrogen Energy. 45 (2020) 10292–10303. https://doi.org/10.1016/j.ijhydene.2019.07.201.

[5] I. Tiseo, Global ethylene demand & capacity 2015-2022, 2020. (2020).

[6] Ethylene prices globally 2021 | Statista, (n.d.).

[7] W. Wu, H. Hu, D. Ding, Low-temperature ethylene production for indirect electrification in chemical production, Cell Reports Phys. Sci. 2 (2021) 100405. https://doi.org/10.1016/j.xcrp.2021.100405.

[8] T.K. Phung, L. Proietti Hernández, A. Lagazzo, G. Busca, Dehydration of ethanol over zeolites, silica alumina and alumina: Lewis acidity, Brønsted acidity and confinement effects, Appl. Catal. A Gen. 493 (2015) 77–89. https://doi.org/10.1016/j.apcata.2014.12.047.

[9] W. Xia, J. Wang, L. Wang, C. Qian, C. Ma, Y. Huang, Y. Fan, M. Hou, K. Chen, Ethylene and propylene production from ethanol over Sr/ZSM-5 catalysts: A combined experimental and computational study, Appl. Catal. B Environ. 294 (2021) 120242. https://doi.org/10.1016/j.apcatb.2021.120242.

[10] U.S Department of Energy, Alternative Fuels Data Center: Maps and Data - Global Ethanol Production by Country or Region, (2021). https://afdc.energy.gov/data/10331 (accessed May 14, 2023).

[11] Federación Nacional de Biocombustibles de Colombia, (n.d.).

[12] Asocaña, Las cifras del sector azucarero colombiano y la producción de bioetanol a base de caña de azúcar, (2017) 1–15.

[13] M.C. Santos, D.F. Costa, A.A. Albuquerque, J.I. Soletti, S.M.P. Meneghetti, Alternative distillation configurations for bioethanol purification: Simulation, optimization and techno-economic assessment, Chem. Eng. Res. Des. 185 (2022) 130–145. https://doi.org/10.1016/j.cherd.2022.06.036.

[14] R.E.N. de Castro, R.M. de B. Alves, C.A.O. do Nascimento, R. Giudici, Assessment

of Sugarcane-Based Ethanol Production, Fuel Ethanol Prod. from Sugarcane. (2018). https://doi.org/10.5772/intechopen.78301.

[15] M.O. de Souza Dias, R. Maciel Filho, P.E. Mantelatto, O. Cavalett, C.E.V. Rossell, A. Bonomi, M.R.L.V. Leal, Sugarcane processing for ethanol and sugar in Brazil, Environ. Dev. 15 (2015) 35–51. https://doi.org/10.1016/j.envdev.2015.03.004.

[16] (UPME) Unidad de Planeación Minero Energética, UPME proyecta entrada de 400 mil vehículos eléctricos para 2030, (2017). https://www1.upme.gov.co/SalaPrensa/ComunicadosPrensa/Comunicado_UPME_10_2017.pdf (accessed February 3, 2022).

[17] J. Becerra, E. Quiroga, E. Tello, M. Figueredo, M. Cobo, Kinetic modeling of polymer-grade ethylene production by diluted ethanol dehydration over H-ZSM-5 for industrial design, J. Environ. Chem. Eng. 6 (2018) 6165–6174. https://doi.org/10.1016/j.jece.2018.09.035.

[18] S. Moon, H.J. Chae, M.B. Park, Dehydration of Bioethanol to Ethylene over H-ZSM-5 Catalysts: A Scale-Up Study, Catal. 2019, Vol. 9, Page 186. 9 (2019) 186. https://doi.org/10.3390/catal9020186.

[19] B. Chen, J. Lu, L. Wu, Z. Chao, Dehydration of bio-ethanol to ethylene over iron exchanged HZSM-5, Chinese J. Catal. 37 (2016) 1941–1948. https://doi.org/10.1016/s1872-2067(16)62524-x.

[20] P. Vondrová, Z. Tišler, J. Kocík, H. de Paz Carmona, M. Murat, Comparison of doped ZSM-5 and ferrierite catalysts in the dehydration of bioethanol to ethylene in a flow reactor, React. Kinet. Mech. Catal. 132 (2021) 449–462.

https://doi.org/10.1007/s11144-021-01925-w/tables/6.

[21] A. Le Valant, F. Can, N. Bion, D. Duprez, F. Epron, Hydrogen production from raw bioethanol steam reforming: Optimization of catalyst composition with improved stability against various impurities, Int. J. Hydrogen Energy. 35 (2010) 5015–5020. https://doi.org/10.1016/j.ijhydene.2009.09.008.

[22] N. Sanchez, R.Y. Ruiz, B. Cifuentes, M. Cobo, Controlling sugarcane press-mud fermentation to increase bioethanol steam reforming for hydrogen production, Waste Manag. 98 (2019) 1–13. https://doi.org/10.1016/j.wasman.2019.08.006.

[23] S. Shetsiri, A. Thivasasith, K. Saenluang, W. Wannapakdee, S. Salakhum, P. Wetchasat, S. Nokbin, J. Limtrakul, C. Wattanakit, Sustainable production of ethylene from bioethanol over hierarchical ZSM-5 nanosheets, Sustain. Energy Fuels. 3 (2018) 115–126. https://doi.org/10.1039/c8se00392k.

[24] C.Y. Wu, H.S. Wu, Ethylene Formation from Ethanol Dehydration Using ZSM-5 Catalyst, ACS Omega. 2 (2017) 4287–4296. https://doi.org/10.1021/acsomega.7b00680.

[25] W. Widayat, A.N. Annisa, Synthesis and Characterization of ZSM-5 Catalyst at Different Temperatures, IOP Conf. Ser. Mater. Sci. Eng. 214 (2017) 012032. https://doi.org/10.1088/1757-899x/214/1/012032.

[26] T.K. Phung, R. Radikapratama, G. Garbarino, A. Lagazzo, P. Riani, G. Busca, Tuning of product selectivity in the conversion of ethanol to hydrocarbons over H-ZSM-5 based zeolite catalysts, Fuel Process. Technol. 137 (2015) 290–297. https://doi.org/10.1016/j.fuproc.2015.03.012.

[27] F.G.H.G. Hashim, Catalytic Reaction of Ethanol into Light Olefins Over 2wt%CuO/HZSM-5, Univ. Technol. 37 (2019) 41–44. https://doi.org/10.30684/etj.37.2b.2.

[28] N. Hadi, A. Niaei, S.R. Nabavi, M. Navaei Shirazi, R. Alizadeh, Effect of second metal on the selectivity of Mn/H-ZSM-5 catalyst in methanol to propylene process, J. Ind. Eng. Chem. 29 (2015) 52–62. https://doi.org/10.1016/j.jiec.2015.03.017.

[29] N. Sanchez, R.Y. Ruiz, B. Cifuentes, M. Cobo, Hydrogen from glucose: A combined study of glucose fermentation, bioethanol purification, and catalytic steam reforming, Int. J. Hydrogen Energy. 41 (2016) 5640–5651. https://doi.org/10.1016/j.ijhydene.2016.01.155.

[30] J.R. Di Iorio, S.A. Bates, A.A. Verma, W.N. Delgass, F.H. Ribeiro, J.T. Miller, R. Gounder, The Dynamic Nature of Brønsted Acid Sites in Cu–Zeolites During NOx Selective Catalytic Reduction: Quantification by Gas-Phase Ammonia Titration, Top. Catal. 2015 587. 58 (2015) 424–434. https://doi.org/10.1007/s11244-015-0387-8.

[31] K.S. Triantafyllidis, L. Nalbandian, P.N. Trikalitis, A.K. Ladavos, T. Mavromoustakos, C.P. Nicolaides, Structural, compositional and acidic characteristics of nanosized amorphous or partially crystalline ZSM-5 zeolite-based materials, Microporous Mesoporous Mater. 75 (2004) 89–100. https://doi.org/10.1016/j.micromeso.2004.07.016.

[32] M. Pérez-Page, J. Makel, K. Guan, S. Zhang, J. Tringe, R.H.R. Castro, P. Stroeve, Gas adsorption properties of ZSM-5 zeolites heated to extreme temperatures, Ceram.

Int. 42 (2016) 15423–15431. https://doi.org/10.1016/j.ceramint.2016.06.193.

[33] E. Quiroga, B. Cifuentes, M. Cobo Angel, Data of the bioethanol dehydration to bioethylene production over doped zeolites, 1 (2023). https://doi.org/10.17632/43DTN3ZMWP.1.

[34] D.T. Sarve, S.K. Singh, J.D. Ekhe, Kinetic and mechanistic study of ethanol dehydration to diethyl ether over Ni-ZSM-5 in a closed batch reactor, React. Kinet. Mech. Catal. 131 (2020) 261–281. https://doi.org/10.1007/s11144-020-01847-z/tables/2.

[35] I. Rossetti, M. Compagnoni, E. Finocchio, G. Ramis, A. Di Michele, Y. Millot, S. Dzwigaj, Ethylene production via catalytic dehydration of diluted bioethanol: A step towards an integrated biorefinery, Appl. Catal. B Environ. 210 (2017) 407–420. https://doi.org/10.1016/j.apcatb.2017.04.007.

[36] J. Yao, S. Liu, G. Chen, W. Yi, J. Liu, Enhanced bioethanol-to-ethylene performance over nanosized sheet-like M-SAPO-34 (M = Sr and K) catalysts, Microporous Mesoporous Mater. 338 (2022) 111980. https://doi.org/10.1016/j.micromeso.2022.111980.

[37] S.P. Banzaraktsaeva, M.A. Surmina, V.A. Chumachenko, E. V. Ovchinnikova, Effect of the Isopropanol Impurity in the Feed on Catalytic Dehydration of Bioethanol to Ethylene, Russ. J. Appl. Chem. 93 (2020) 721–728. 1 https://doi.org/10.1134/s1070427220050134.

[38] N. Zhan, Y. Hu, H. Li, D. Yu, Y. Han, H. Huang, Lanthanum–phosphorous modified HZSM-5 catalysts in dehydration of ethanol to ethylene: A comparative analysis,

Catal. Commun. 11 (2010) 633–637. https://doi.org/10.1016/J.CATCOM.2010.01.011.

[39] A. Chaibi, Y. Boucheffa, N. Bendjaballah-Lalaoui, TGA investigation of water and ethanol adsorption over LTA zeolites, Microporous Mesoporous Mater. 324 (2021) 111285. https://doi.org/10.1016/j.micromeso.2021.111285.

[40] M.A. Oliver-Tolentino, A. Guzmán-Vargas, E.M. Arce-Estrada, D. Ramírez-Rosales, A. Manzo-Robledo, E. Lima, Understanding electrochemical stability of Cu+ on zeolite modified electrode with Cu-ZSM5, J. Electroanal. Chem. 692 (2013) 31–39. https://doi.org/10.1016/j.jelechem.2012.12.015.

[41] C. Wu, H. Guo, S. Cui, H. Li, F. Li, Influence of Ce doping on structure, morphology, and photocatalytic activity of three-dimensional ZnO superstructures synthesized via coprecipitation and roasting processes, J. Nanoeng. Nanosyst. 229 (2014) 66–73. https://doi.org/10.1177/1740349914526867.

[42] A. Zachariou, A.P. Hawkins, R.F. Howe, J.M.S. Skakle, N. Barrow, P. Collier, D.W. Nye, R.I. Smith, G.B.G. Stenning, S.F. Parker, D. Lennon, Counting the Acid Sites in a Commercial ZSM-5 Zeolite Catalyst, ACS Phys. Chem. Au. 3 (2023) 74–83. https://doi.org/10.1021/acsphyschemau.2c00040.

[43] L. Ouayloul, M. El Doukkali, M. Jiao, F. Dumeignil, I. Agirrezabal-Telleria, New mechanistic insights into the role of water in the dehydration of ethanol into ethylene over ZSM-5 catalysts at low temperature, Green Chem. 25 (2023) 3644–3659. https://doi.org/10.1039/d2gc04437d.

[44] T.K. Phung, G. Busca, Ethanol dehydration on silica-aluminas: Active sites and

ethylene/diethyl ether selectivities, Catal. Commun. 68 (2015) 110–115. https://doi.org/10.1016/j.catcom.2015.05.009.

[45] H. Khezri, A. Izadbakhsh, A.A. Izadpanah, Promotion of the performance of La, Ce and Ca impregnated HZSM-5 nanoparticles in the MTO reaction, Fuel Process. Technol. 199 (2020) 106253. https://doi.org/10.1016/j.fuproc.2019.106253.

[46] L. Sun, X. Guo, G. Xiong, X. Wang, Ethylation of coking benzene with ethanol over nano-sized ZSM-5 zeolites: Effects of rare earth oxides on catalyst stability, Catal. Commun. 25 (2012) 18–21. https://doi.org/10.1016/j.catcom.2012.03.036.

[47] J. Wan, F. Chang, Y. Wei, Q. Xia, Z. Liu, Mechanistic studies on the coupled reaction of n-Hexane and ethanol over HZSM-5 zeolite catalyst, Catal. Letters. 127 (2009) 348–353. https://doi.org/10.1007/s10562-008-9687-y.

[48] P. Tynjälä, T.T. Pakkanen, Modification of zsm-5 zeolite with trimethyl phosphite part 1. structure and acidity, Microporous Mesoporous Mater. 20 (1998) 363–369. https://doi.org/10.1016/S1387-1811(97)00050-4.

[49] Z. Liu, J. Li, Y. Tan, L. Guo, Y. Ding, Copper Supported on MgAlOx and ZnAlOx Porous Mixed-Oxides for Conversion of Bioethanol via Guerbet Coupling Reaction, Catalysts. 12 (2022). https://doi.org/10.3390/catal12101170.

[50] T.K. Phung, G. Busca, Diethyl ether cracking and ethanol dehydration: Acid catalysis and reaction paths, Chem. Eng. J. 272 (2015) 92–101. https://doi.org/10.1016/j.cej.2015.03.008.

[51] Z.S.B. Sousa, D. V. Cesar, C.A. Henriques, V. Teixeira Da Silva, Bioethanol conversion into hydrocarbons on HZSM-5 and HMCM-22 zeolites: Use of in situ

DRIFTS to elucidate the role of the acidity and of the pore structure over the coke formation and product distribution, Catal. Today. 234 (2014) 182–191. https://doi.org/10.1016/J.CATTOD.2014.03.023.

[52] Y. Hao, D. Zhao, Y. Zhou, M. Yin, Z. Wang, G. Xi, S. Song, Q. Tang, J.H. Yang, Hierarchical leaf-like alumina-carbon nanosheets with ammonia water modification for ethanol dehydration to ethylene, Fuel. 333 (2023) 126128. https://doi.org/10.1016/j.fuel.2022.126128.

[53] P. Pornsetmetakul, S. Klinyod, C. Rodaum, S. Salakhum, P. Iadrat, E.J.M. Hensen, C. Wattanakit, Fine-Tuning Texture of Highly Acidic HZSM-5 Zeolite for Efficient Ethanol Dehydration, ChemCatChem. 15 (2023). https://doi.org/10.1002/cctc.202201387.

[54] R. Le Van Mao, T.M. Nguyen, J. Yao, Conversion of ethanol in aqueous solution over ZSM-5 zeolites: Influence of Reaction Parameters and Catalyst Acidic Properties as Studied by Ammonia TPD Technique, Appl. Catal. 61 (1990) 161–173. https://doi.org/10.1016/S0166-9834(00)82141-7.

[55] D. Masih, S. Rohani, J.N. Kondo, T. Tatsumi, Catalytic dehydration of ethanol-to-ethylene over Rho zeolite under mild reaction conditions, Microporous Mesoporous Mater. 282 (2019) 91–99. https://doi.org/10.1016/j.micromeso.2019.01.035.

[56] Y.W. Cheng, C.C. Chong, C.K. Cheng, K.H. Ng, T. Witoon, J.C. Juan, Ethylene production from ethanol dehydration over mesoporous SBA-15 catalyst derived from palm oil clinker waste, J. Clean. Prod. 249 (2020) 119323. https://doi.org/10.1016/j.jclepro.2019.119323.

[57] J. Liu, C. Zhang, Z. Shen, W. Hua, Y. Tang, W. Shen, Y. Yue, H. Xu, Methanol to propylene: Effect of phosphorus on a high silica HZSM-5 catalyst, Catal. Commun. 10 (2009) 1506–1509. https://doi.org/10.1016/j.catcom.2009.04.004.

[58] B. Cifuentes, M.F. Valero, J.A. Conesa, M. Cobo, Hydrogen Production by Steam Reforming of Ethanol on Rh-Pt Catalysts: Influence of CeO_2, ZrO_2, and La_2O_3 as Supports, Catal. 2015, Vol. 5, Pages 1872-1896. 5 (2015) 1872–1896. https://doi.org/10.3390/catal5041872.

[59] E.A. Skiba, O. V. Baibakova, V. V. Budaeva, I.N. Pavlov, M.S. Vasilishin, E.I. Makarova, G. V. Sakovich, E. V. Ovchinnikova, S.P. Banzaraktsaeva, N. V. Vernikovskaya, V.A. Chumachenko, Pilot technology of ethanol production from oat hulls for subsequent conversion to ethylene, Chem. Eng. J. 329 (2017) 178–186. https://doi.org/10.1016/j.cej.2017.05.182.

CRediT authorship contribution statement

Eliana Quiroga. Methodology, Validation, Formal Analysis, Research, Data Processing, Writing-Original Draft, Visualization. **Nicolas García.** Validation, Formal Analysis, Research, Data Processing, Writing-Original Draft, Visualization. **Bernay Cifuentes.** Formal Analysis, Data Processing, Writing-Original Draft, Writing-Revision and Editing, Visualization. **Ricardo Cogua.** Methodology, Research, Data Processing**. Jorge Becerra.** Formal Analysis, Writing-Revision and Editing. **Julia Moltó:** Resources, Supervision, Research, Data processing, Fund Acquisition. **Martha Cobo.** Conceptualization, Methodology, Formal Analysis, Resources, Writing-Revision and Editing, Supervision, Project Management, Fund Acquisition.

Declaration of Competing Interest

☒ The authors declare that they have no known competing financial interests or personal relationships that could have appeared to influence the work reported in this paper.

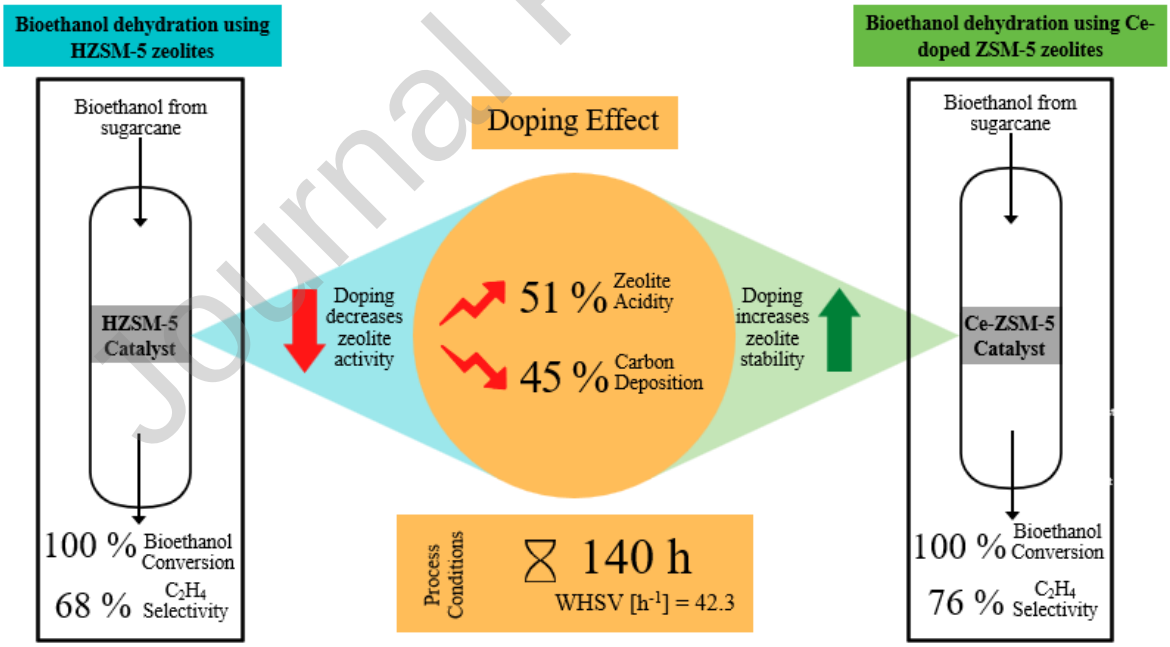

Graphical Abstract

Highlights

- Catalytic dehydration of industrial crude bioethanol over H-ZSM-5 was assessed
- Although doping decreases zeolite activity, it increases stability
- H-ZSM-5 with Si/Al of 26 reaches 100% conversion and 68% selectivity for 140 h TOS
- When doping with Ce, it maintains conversion and increases selectivity up to 76% for 140 h TOS